JOURNAL DE PHYSIQUE
Colloque C4, supplément au n° 12, Tome 43, décembre 1982 *page* C4-819

COHERENCY OF THE TRANSFORMATION STRAIN AT THE GRAIN BOUNDARY AND FRACTURE IN Cu-Zn-Al ALLOY

K. Takezawa, T. Izumi, H. Chiba and S. Sato

Department of Applied Physics, Faculty of Engineering, Hokkaido University, Sapporo, 060, Japan

(Accepted 9 August 1982)

Abstract.- Two types of Cu-Zn-Al bicrystal specimens having e/a≃1.4, one with the boundary parallel to and the other perpendicular to the tensile direction, were extended at room temperature. The morphological change near the boundary was continuously observed by a microscope with a VTR during the extension. For a particular orientation with respect to the tensile direction, the same variant crystal of β_1' martensite as that which would be stress-induced in an individual component crystal is produced with transformation strains which occasionally continue across the boundary. However, a different variant crystal from that in the individual component crystal is usually formed near the boundary depending on the orientation of the other grain. This variant has an orientation such that the strain fields coincide with those produced by a variant which is transformed simultaneously in the other grain near the boundary. Since the possible number of shear systems producing the intimate β_1' variants in both grains is limited, the fracture takes place often at the grain boundary. However, when α_1' martensites are formed at the boundary, as frequently observed, the fracture is suppressed to a great extent, because of increasing numbers of independent shear systems. Consequently, the degree of ease or difficulty in producing α_1' martensites is closely associated with the character of fracture in Cu-Zn-Al alloy. An extended work on fracture using polycrystalline specimens of different e/a values also supported the above results.

Introduction.- The mechanical behavior associated with the shape memory effect and pseudoelasticity in polycrystalline Cu-base martensitic alloys is remarkably affected by the size and crystallographic orientations of the individual grains[1, 2]. This is because the grain boundary has the life-and-death power over the reversibility of martensitic transformation and therefore the investigation concerning the effect of boundary[3, 4] is unavoidable work prior to the industrial use of these phenomena. In the present work a detailed morphological examination was performed on various bicrystals of Cu-Zn-Al alloys with different orientations of component crystals. Attension was paid to the strain compatibility of the stress-induced

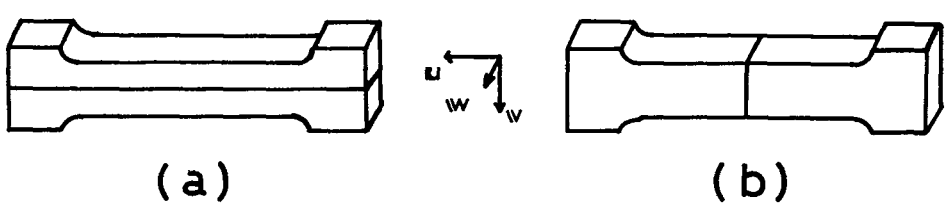

Fig. 1 Two types of bicrystal tensile specimens.
(a) Type A (equi-strain) (b) Type B (equi-stress).

martensite at the boundary. As reported so far[5], since the transformation proceeds by two steps in this alloy system, i.e., $\beta_1 \rightarrow \beta_1' \rightarrow \alpha_1'$, the behavior of not only β_1' but also α_1' martensites has been studied in relation to the facture at the boundary.

Experimental procedure.- Ingots of Cu-Zn-Al alloys with various compositions were prepared from high purity Cu, Zn and Al by melting at 1373 K in argon filled silica capsules. The melts were slowly cooled to 1143 K and homogenized for 1 hr at this temperature, followed by quenching. The grain size of the ingot was large enough to prepare bicrystal tensile specimens. Two types of bicrystal specimens, one with the boundary parallel to (type A, equi-strain) and the other perpendicular to (type B, equi-stress) the tensile direction were cut from the ingot by a spark machine as shown in Fig. 1. The compositions of alloys were set so as to keep the Ms temperature constant, i.e. 260 K, using an empirical formula of $Ms\,(K)=3350-80C_Z-110C_A$, where C_Z and C_A are the concentration of Zn and Al, respectively. Polycrystalline tensile specimens with different compositions were also prepared. The morphological change near the boundary was continuously observed by a microscope with a VTR during the extension of the specimen by an Instron type machine, the stress-strain curve being recorded as well.

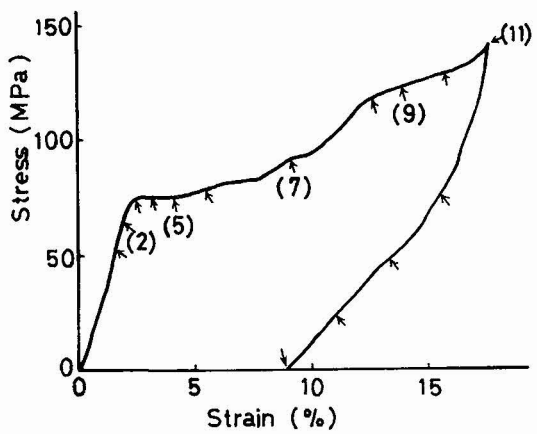

Fig. 2 Stress-strain curve for a Type A bicrystal specimen of Cu-31.6at% Zn-4.2at%Al alloy. The tensile directions are $[9\bar{4}\bar{2}]$ and $[5\bar{2}0]$, for component crystals, respectively.

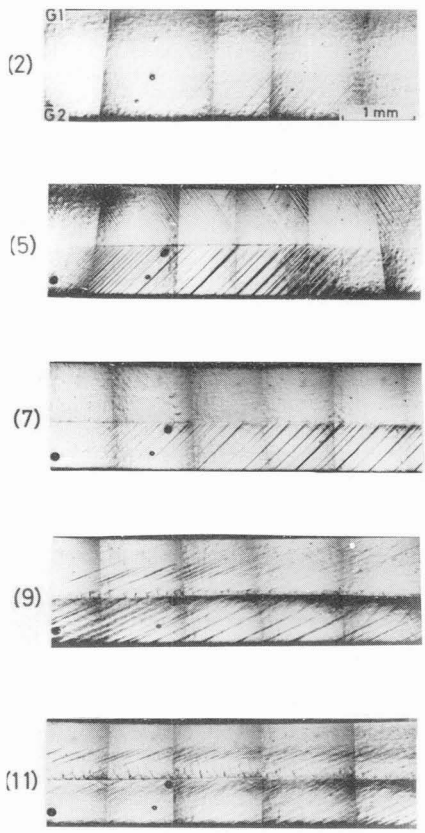

Photo.1 Change in macrographic structure upon loading. The macrographs were taken at the points numbered in Fig. 2.

Results and discussion.- Fig. 2 shows an example of the stress-strain curves obtained for a type A bicrystal specimen of Cu-31.6at%Zn-4.2at% Al alloy. The tensile directions with respect to the component crystals, grain No. 1(G1) and No. 2(G2), were $[9\bar{4}\bar{2}]$ and $[5\bar{2}0]$, respectively. The numbers in the figure indicate the points where macrographs were taken for the morphological examination as shown in Photo. 1. As clearly observed in Photo. 1, as soon as a β_1' variant was induced in the bottom grain, G2, at the point (2), another β_1' appeared in the other grain, G1, and these β_1' variant crystals in both grains grew cooperatively with a similar rate up to (5). At (7) the first transformation was completed in G1 and the second one, $\beta_1' \rightarrow \alpha_1'$, started to appear in β_1' with new traces, and as increasing stress the number of α_1' traces was increased in both grains. Moreover, one sees zig-zag slip lines in G1 near the boundary at (9). These lines locate only near the boundary even at higher stress level (11).

The most important feature in this type of morphological change is that the martensitic transformation does not take place independently in both grains but proceeds with strong interference across the boundary. This is caused by a necessary condition associated with the compatibility of transformation strains at the grain boundary. When the condition can not be fulfilled completely, a slip deformation must be operated as seen in Photo. 1(9). The condition of strain compatibility is to have the same value of strain components, ε_{uu}, ε_{ww} and γ_{uw} in both grains for type A (equi-strain) specimen and of ε_{vv}, ε_{ww} and γ_{vw} for type B (equi-stress) specimen, respectively, when we take u, v and w axes as shown in Fig. 1 [6, 7].

Photo. 2 is a macrograph showing homogenuously distributed β_1' martensite in both grains. The specimen contains 4.2at%Al as well, and the tensile directions of component crystals, G1 and G2, are $[5\bar{4}1]$ and $[13\bar{1}0\bar{2}]$, respectively. Two variant crystals, having $(12\bar{2}11)$ habit plane in G1 and $(12\bar{2}\bar{1}\bar{1})$ in G2 stick together one by one at the boundary. The strain components, ε_{uu}, ε_{ww} and γ_{uw}, are calculated to be 0.075x, -0.021x and -0.041x for the first martensite in G1 and 0.069x, -0.019x and -0.053x for the second one in G2, respectively, where x means the fractional volume of β_1'. One sees very good strain compatibility in this case. It is interesting that a calculation derives a smaller value of Schmid factor, 0.37, for the variant appeared in G2 having $(12\bar{2}\bar{1}\bar{1})$ habit plane than that of 0.39 for a variant having $(12\bar{2}11)$ habit plane. This means that a different variant from that which would be stress-induced in G2 was transformed by the strain compatibility at the boundary.

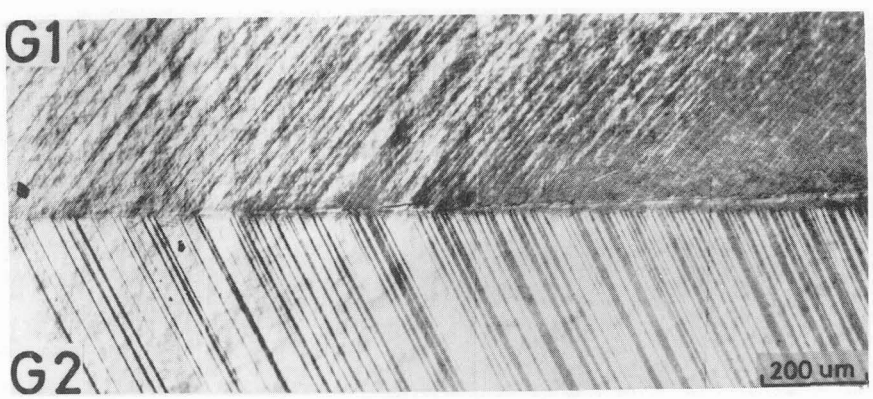

Photo. 2 A macrograph showing homogeneously distributed β_1' martensites in both grains of type A specimen. They meet one by one at the boundary.

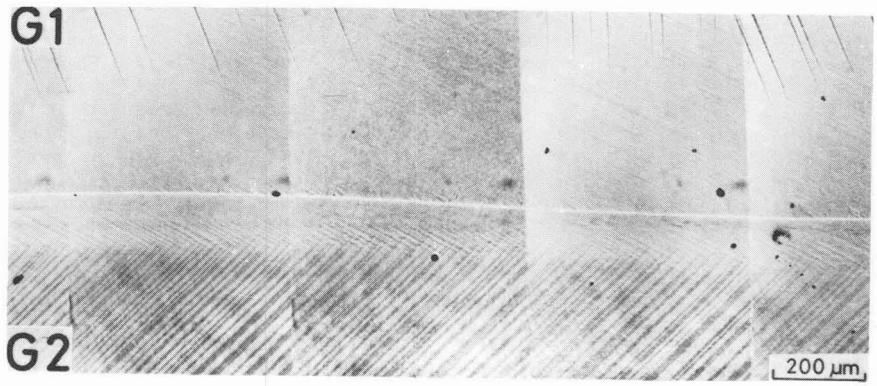

Photo. 3 A macrograph showing complex structure near the boundary. Different variant crystals of β_1' martensite from those with maximum Schmid factor were induced near the boundary in both grains. α_1' martensites are also seen.

A more striking example of the above phenomenon is represented in Photo. 3. The tensile directions were $[9\,\bar{4}\,\bar{1}]$ and $[4\,\bar{2}\,\bar{1}]$ for G1 and G2, respectively. Initially, a small amount of β_1' martensites having maximum Schmid factors, i.e., with $(12\,\bar{2}\,11)$ habit planes, were introduced in both grains except near the boundary. However, since the shear components of the transformation strain of these martensites were quite diffrent in both grains, i.e., -0.006x in G1 and 0.044x in G2, a new variant of β_1' martensite having $(12\,11\,\bar{2})$ habit plane, which had γ_{uw}=0.027x, appeared near the boundary instead of the former one in G1 and grew with increasing applied stress. Furthermore, following to the growth of this variant, the second transformation $\beta_1' \rightarrow \alpha_1'$ took place at the boundary in G2 as seen in Photo. 3.

The behavior of stress-induced transformation in bicrystal of type A (equi-strain) is strongly affected by the grain boundary as described above. On the other hand, in the case of type B bicrystal, the component crystals behave as if each crystal were individually elongated, except the region near the boundary. So that, in this case the variant crystal of β_1' martensite was the same as that in a single crystal of each component and the stress-strain curve becomes simply a superposed curve of the two individual stress-strain curves of component crystals. At the grain boundary, except for a particular orientation relation between two component crystals, complex morphological behaviors are generaly observed by the strain compatibility. In bicrystal specimens with 31.6at%Zn and 4.2at%Al, as the applied stress was increased, the α_1' martensites were quite often observed near the grain boundary with a number of slip traces inside. However, cracks were formed easily at the boundary for specimens containing higher Al contents, independent of the type of bicrystal, in which the second transformation was hardly generated.

In Fig. 3 are shown stress-strain curves up to fracture for specimens of single crystal, bicrystal and polycrystal of two kinds of alloy with different Al contents. The curve (a) obtained for a single crystal of 4.2at%Al alloy indicates a large elongation of 20% corresponding to the $\beta_1 \rightarrow \beta_1' \rightarrow \alpha_1'$ transformation which was followed by an additional 25% plastic deformation by slip in the α_1' martensite. The surface of fracture showed a typical pattern of the ductile fracture. The curve (b) was recorded for a specimen of type A bicrystal having a particular orientation relation of component crystals such that the β_1' martensites with maximum Schmid factor induced in both grains were well connected with each other as shown in Photo. 2. The elongation was reached up to 60% at the fracture. In this case, the martensites

were introduced quite homogeneously in the specimen and slip traces of $\{111\}_{\alpha_1'}$ were distributed uniformly in two directions. It seems possible to understand that the boundary parallel to the tensile direction plays a roll to keep homogeneous deformations in the specimen. The result that the value of fracture strain in bicrystal in (b) was larger than that in (a) of single crystal is thought to be originated by the homogeneity in deformation associated with the formation of α_1' martensite. Contrary to this, for a type B specimen of bicrystal, it is supposed that the grain boundary might operate so as to increase inhomogeneous deformations in the specimen, because it produces a specially deformed cross-sectional region in the specimen. In fact, the fracture strains in type B specimens were always smaller than those in single crystals.

One sees a quite different stress-strain curve for a type A bicrystal specimen containing 15% Al as in (d). In this alloy, only the $\beta_1 \rightarrow \beta_1'$ transformation took place and no remarkable slip deformation was introduced. The fracture occurred at an elongation of only 10% and the fracture surface showed a pattern of brittle fracture. A separate measurement [8] showed that the critical resolved shear stress (CRSS) for the $\beta_1' \rightarrow \alpha_1'$ transformation, τ_α, was almost independent of temperature but strongly depended on the composition in alloys. An example of measured τ_α for

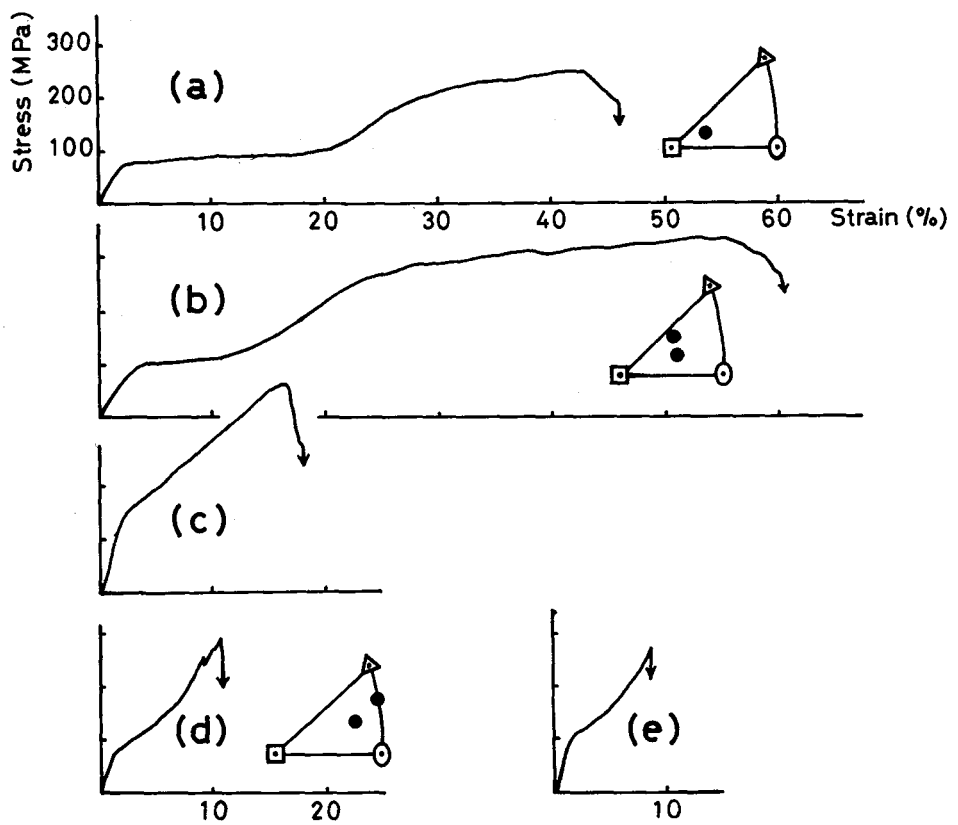

Fig. 3 Stress-strain curves with different fracture strain.
(a) Single crystal of Cu-31.6at%Zn-4.2at%Al alloy.
(b) Bicrystal of Cu-31.6at%Zn-4.2at%Al alloy.
(c) polycrystal of Cu-31.6at%Zn-4.2at%Al alloy.
(d) Bicrystal of Cu-16.7at%Zn-15.0at%Al alloy.
(e) Polycrystal of Cu-16.7at%Zn-15.0at%Al alloy.

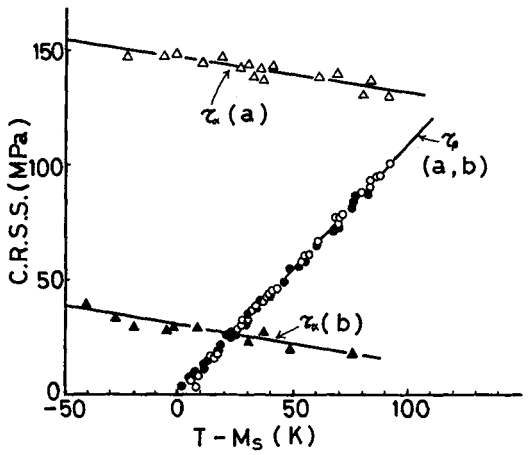

Fig. 4

Variation of critical resolved shear stress for transformation in two Cu-Zn-Al alloys. τ_β and τ_α are the CRSS for $\beta_1 \rightarrow \beta_1'$ and $\beta_1' \rightarrow \alpha_1$ transformations, respectively. (a) Cu-19.5at%Zn-13.0at%Al alloy. (b) Cu-31.8at%Zn-4.0 at%Al alloy.

Cu-31.8at%Zn-4.0at%Al (e/a=1.398, Ms=263°K) and Cu-19.5at%Zn-13.0at%Al alloy (e/a=1.455, Ms=263°K) is represented in Fig. 4 accompanying with the values of τ_β, CRSS for $\beta_1 \rightarrow \beta_1'$, at different temperatures. The above data on CRSS clearly support that the observed fracture in Fig. 3 (d) can be attributed to the lack of α_1' martensite at the boundary. Fig. 3 (c) and (e) are the stress-strain curves for polycrystalline specimens with low and high Al contents, respectively. The fracture strain in (c) was apparently larger than in (e) as expected.

It is concluded in the present study that the behavior of stress-induced transformation is greatly affected by the strain compatibility at the grain boundary in Cu-Zn-Al alloys. Moreover, it was found that the formation of α_1' martensite played an important role to attain the strain compatibility and to avoid the fracture at the boundary. Even though the cutting of β_1' martensites is difficult to occur in general, a pair of special variant crystals of β_1' can cross each other to form α_1' martensite as reported previously [5], the phenomenon being closely related to the appearance of the reversible shape memory effect in Cu-Zn-Al alloys [9]. It is strongly dependent on the value of τ_α whether or not the crossing of the β_1' martensite can easily occur. So that, in alloys with high Al contents, only one variant of β_1' martensite can usually be formed at the boundary. Since possible shear systems are limitted there, because of the crystal structure of 9R, the stress is hardly reliesed. On the other hand, in alloys with low Al contents, not only a pair of variant β_1' in both grains can be induced but also α_1' martensites are formed easily at the boundary. Consequently, the number of possible shear systems is increased by adding four $\{111\}\langle 110\rangle_{\alpha_1}$ slip systems of α_1' martensite and the strain compatibility can become attained more easily.

References

[1] Dvorak(I.) and Hawbolt(E.B.), Met. Trans. 6A (1975) 95.
[2] Schroeder(T.A.), Cornelis(I.) and Wayman(C.M.), Met. Trans. 7A (1976) 535.
[3] Wield(D.V.), and Gillam(E.), Acta Met. 25 (1977) 725.
[4] Miyazaki(S.), Otsuka(K.), Sakamoto(H.) and Shimizu(K.), Trans. JIM 22 (1981) 244.
[5] Sato(H.), Takezawa(K.), Sato(S.), Proc. Joint US/Japan Seminar, Troy, N.Y., U.S.A. (1979) 92.
[6] Livingston(J.D.) and Chalmers(B.), Acta Met. 5 (1957) 322.
[7] Hirth(J.P.) and Lothe(J.), Theory of Dislocations, McGraw-Hill Inc. (1968) 284.
[8] Sato(H.), Takezawa(K.) and Sato(S.), Sci. Rep. RITU, Suppl. 1 A29 (1981) 85.
[9] Takezawa(K.) and Sato(S.), Proc. Intern. Conf. on Martensitic Transformations, ICOMAT-79 (1979) 655.